Steric Effects of Meta Substituents in Substituted Tetraphenylporphyrin Complexes of Ruthenium, Indium, Titanium, and Gallium

A. Laurie W. Shroyer, Charles Lorberau, and Sandra S. Eaton*[1]

Department of Chemistry, University of Colorado at Denver, Denver, Colorado 80202

Gareth R. Eaton

Department of Chemistry, University of Denver, Denver, Colorado 80208

Received April 9, 1980

The ruthenium carbonyl 4-*tert*-butylpyridine, indium chloride, titanyl, and gallium chloride complexes of tetrakis(3,4,5-trimethoxyphenyl)porphyrin and tetrakis(3,5-dimethoxyphenyl)porphyrin and the ruthenium carbonyl 4-*tert*-butylpyridine, titanyl, and gallium chloride complexes of tetrakis(3,5-di-*tert*-butyl-4-hydroxyphenyl)porphyrin and tetrakis(3,5-di-*tert*-butyl-4-methoxyphenyl)porphyrin have been prepared. For each metal ion, the electronic spectra were used to monitor the electronic effects of the porphyrin substituents. Rates of phenyl ring rotation were obtained from the variable-temperature ^{1}H NMR spectra of the ortho protons and of the meta substituents. The rate of exchange between free 4-*tert*-butylpyridine and 4-*tert*-butylpyridine coordinated to the ruthenium complexes was obtained from the ^{1}H NMR spectra of the *tert*-butyl groups. The rates of phenyl ring rotation in the meta-substituted complexes are 7–10 times slower than those expected on the basis of the previously observed electronic effects on phenyl ring rotation. Rates of 4-*tert*-butylpyridine exchange are 2–3 times faster than those expected on the basis of electronic effects. The reduced rate of phenyl ring rotation and the enhanced rate of 4-*tert*-butylpyridine exchange are attributed to a steric effect of the meta substituents.

Recent studies of the rates of phenyl ring rotation in metal complexes of para-substituted tetraphenylporphyrins have examined the effect of both the metal ion and the para substituent.[2,3] The results indicate that the effect of the para substituent on the rate of phenyl ring rotation is largely electronic in nature whereas the effect of metal ion is primarily steric. For elucidation of the importance of both steric and electronic factors in determining the rate of phenyl ring rotation, this paper reports the study of a series of meta-substituted porphyrins. Rates of phenyl ring rotation have been obtained for the complexes 1, obtained from H_2(OMe_2-TPP) (R_3, R_5 = OMe,

R_4 = H) and H_2(OMe_3-TPP) (R_3 = R_4 = R_5 = OMe) with MXY = Ru(CO)(*t*-Bupy), InCl, TiO, and GaCl and the complexes obtained from H_2(tBu_2OH-TPP) (R_3 = R_5 = *t*-Bu, R_4 = OH) and H_2(*t*-Bu_2OMe-TPP) (R_3 = R_5 = *t*-Bu, R_4 = OMe) with MXY = Ru(CO)(*t*-Bupy), TiO, and GaCl.[4] The rate of exchange between free and coordinated 4-*tert*-butylpyridine has also been studied for the ruthenium complexes.

The analysis of the effects of the meta sustituents includes a comparison with data previously obtained for para-substituted complexes. The combined results include ring-rotation data for 39 metalloporphyrins and *t*-Bupy-exchange data for 10 ruthenium porphyrins.

Experimental Section

Physical Measurements. Visible spectra were obtained in chloroform solutions on a Beckman Acta V spectrometer. Data are given below with wavelengths in nanometers and log ϵ values in parentheses. Infrared spectra were recorded as Nujol or halocarbon mulls on a Perkin-Elmer 237 or 710 spectrometer. ^{1}H NMR spectra were run at power levels well below saturation on a Varian HA-100 spectrometer equipped with a variable-temperature probe. Spectra were run on 1,1,2,2-tetrachloroethane ($C_2H_2Cl_4$) or 1:3 trichloroethylene–tetrachloroethane solutions with the spectrometer locked on the $C_2H_2Cl_4$ resonance. ^{1}H NMR chemical shifts were measured with respect to $C_2H_2Cl_4$ and are reported in parts per million downfield of Me_4Si at room temperature (unless otherwise noted) with a correction of 5.96 ppm for the chemical shift of $C_2H_2Cl_4$.

Preparation of Compounds. Unless otherwise noted, all reagents were commercially available and were used without purification.

Porphyrins. The porphyrins were prepared by condensation of a substitued benzaldehyde and pyrrole in propionic acid by the method of Adler[5] and purified by chromatography on Baker 0537 alumina with $CHCl_3$ as eluant. Characterization data are given below for the individual compounds.

Tetrakis(3,5-dimethoxyphenyl)porphyrin, H_2(OMe_2-TPP): yield 17.5%; visible spectrum 421 (5.72), 516 (4.36), 550 (3.78), 590 (3.81), 646 (3.56); ^{1}H NMR ($CDCl_3$) 8.92 (s, pyrrole H), 7.40 (d, J = 2.3 Hz, *o*-H), 6.90 (t, J = 2.3 Hz, *p*-H), 3.94 (s, *m*-OMe), −2.81 (br, NH, disappeared when D_2O was added). Anal. Calcd for $C_{52}H_{46}N_4O_8$: C, 73,05; H, 5.42; N, 6.55. Found: C, 72.87; H, 5.43; N, 6.54.

Tetrakis(3,4,5-trimethoxyphenyl)porphyrin, H_2(OMe_3-TPP): yield 21%; visible spectrum 407 (sh, 4.61), 424 (5.70), 517 (4.33), 554 (3.92), 590 (3.79), 648 (3.63); ^{1}H NMR ($CDCl_3$) 8.96 (s, pyrrole H), 7.48 (s, *o*-H), 3.98 (s, *m*-OMe), 4.18 (s, *p*-OMe), −2.75 (br, NH, disappeared when D_2O was added). Anal. Calcd for $C_{56}H_{54}N_4O_{12}$: C, 68.98; H, 5.58; N, 5.75. Found: C, 68.95; H, 5.52; N, 5.78.

Tetrakis(3,5-di-*tert*-butyl-4-hydroxyphenyl)porphyrin, H_2(*t*-Bu_2OH-TPP): yield 13%; visible spectrum 409 (sh, 4.87), 426 (5.69), 523 (4.22), 561 (4.17), 595 (3.74), 653 (3.94); IR ν_{OH} 3760, ν_{NH} 3430 cm^{-1}; ^{1}H NMR ($CDCl_3$) 8.90 (s, pyrrole H), 8.04 (s, *o*-H), 5.48 (s, *p*-OH), 1.52 (s, *m*-*t*-Bu), −2.60 (b, NH). The signals at δ 5.48 and −2.60 disappeared when D_2O was added. Anal. Calcd for $C_{76}H_{94}N_4O_4$: C, 80.95; H, 8.40; N, 4.97. Found: C, 80.77; H, 8.53; N, 4.95.

Tetrakis(3,5-di-*tert*-butyl-4-methoxyphenyl)porphyrin, H_2(*t*-Bu_2OMe-TPP). The aldehyde group in 3,5-di-*tert*-butyl-4-hydroxybenzaldehyde was protected by reaction with ethylene glycol.[6] The hydroxy group was methylated[7] and the

(1) Author to whom correspondence should be addressed. On sabbatical, 1979–1980, University of Denver.

(2) Eaton, S. S.; Eaton, G. R. *J. Am. Chem. Soc.* **1977**, *99*, 6594–9.

(3) Eaton, S. S.; Fishwild, D. M.; Eaton, G. R. *Inorg. Chem.* **1978**, *17*, 1542–5.

(4) Abbreviations used throughout: *t*-Bupy, 4-*tert*-butylpyridine; *p*-R-TPP, tetrakis(*p*-R-phenyl)porphyrin dianion; OMe_2-TPP, tetrakis(3,5-dimethoxyphenyl)porphyrin dianion; OMe_3-TPP, tetrakis(3,4,5-trimethoxyphenyl)porphyrin dianion; *t*-Bu_2OH-TPP, tetrakis(3,5-di-*tert*-butyl-4-hydroxyphenyl)porphyrin dianion; *t*-Bu_2OMe-TPP, tetrakis(3,5-di-*tert*-butyl-4-methoxyphenyl)porphyrin dianion.

(5) Adler, A. D.; Longo, F. R.; Finarelli, J. D.; Goldmacher, J.; Assour, J.; Korsafkoff, L. *J. Org. Chem.* **1967**, *32*, 476.

(6) Anderson, L. C.; Pinnick, H. W. *J. Org. Chem.* **1978**, *43*, 3417–8.

0022-3263/80/1945-4296$01.00/0

protecting group removed by stirring the mixture in 25:1 acetone–H_2O solution with *p*-toluenesulfonic acid as catalyst. The product was distilled at 140 °C (5 mm): yield 78%; IR ν_{CO} 1700 cm^{-1}; ^1H NMR ($CDCl_3$) 9.89 (s, aldehydic H), 7.82 (s, *o*-H), 3.74 (s, OCH_3), 1.47 (s, *t*-Bu). The aldehyde was reacted with pyrrole by the method of Adler:[5] yield 19%; visible spectrum 651 (3.92), 595 (3.78), 559 (4.15), 521 (4.30), 492 (sh, 3.70), 424 (5.77), 406 (4.95); IR ν_{NH} 3330 cm^{-1}; ^1H NMR ($CDCl_3$) 8.92 (s, pyrrole H), 8.12 (s, *o*-H), 3.98 (s, *p*-OMe), 1.64 (s, *m*-*t*-Bu), −2.66 (br, NH). Anal. Calcd for $C_{80}H_{102}N_4O_4$: C, 81.17; H, 8.69; N, 4.73. Found: C, 81.13; H, 8.52; N, 4.80.

Ruthenium Complexes. The ruthenium complexes were prepared by the method reported for Ru(CO)(*p*-R-TPP)(L)[8] and purified by chromatography on Baker 0537 alumina. After removal of the chromatographic solvent, the product was dissolved in C_2HCl_3, and excess *t*-Bupy was added. After the mixture was boiled for 15 min, hexane was added and the product crystallized. Details of the chromatography conditions and characterization data for individual complexes are given below.

Ruthenium Carbonyl Tetrakis(3,5-dimethoxyphenyl)porphyrin 4-*tert*-Butylpyridine, Ru(CO)(OMe_2-TPP)(*t*-Bupy). The reaction time was 16 h. Activity III alumina was used for the chromatography. CH_2Cl_2 was used to elute impurities, and the complex was eluted with 20:1 CH_2Cl_2–THF: yield 66%; visible spectrum 415 (5.45), 533 (4.34), 570 (3.50); IR ν_{CO} 1955 cm^{-1}; ^1H NMR 8.70 (s, pyrrole H), 7.42, 7.19 (m, *o*-H), 6.84 (t, J = 2.3 Hz, *p*-H), 3.94, 3.96 (s, *m*-OMe), 5.12 (d, J = 6.5 Hz, *t*-Bupy β-H), 1.37 (d, J = 6.5 Hz, *t*-Bupy α-H), 0.34 (s, *t*-Bupy *t*-Bu). Anal. Calcd for $C_{62}H_{57}N_5O_9Ru$: C, 66.65; H, 5.14; N, 6.27. Found: C, 66.54; H, 5.06; N, 6.35.

Ruthenium Carbonyl Tetrakis(3,4,5-trimethoxyphenyl)porphyrin 4-*tert*-Butylpyridine, Ru(CO)(OMe_3-TPP)(*t*-Bupy). The reaction time was 4 h. Activity IV alumina was used for the chromatography. Impurities were eluted with CH_2Cl_2 containing 1% THF, and the product was eluted with 5:1 CH_2Cl_2–THF: yield 70%; visible spectrum 417 (5.44), 534 (4.34), 568 (3.68); IR ν_{CO} 1935 cm^{-1}; ^1H NMR 8.71 (s, pyrrole H), 7.45, 7.25 (d, J = 1.6 Hz, *o*-H), 3.95, 3.92 (s, *m*-OMe), 4.08 (s, *p*-OMe), 5.22 (d, *t*-Bupy β-H), 1.47 (d, *t*-Bupy α-H), 0.35 (s, *t*-Bu). Anal. Calcd for $C_{66}H_{65}N_5O_{13}Ru$: C, 64.07; H, 5.29; N, 5.66. Found: C, 63.84; H, 5.24; N, 5.67.

Ruthenium Carbonyl Tetrakis(3,5-di-*tert*-butyl-4-hydroxyphenyl)porphyrin 4-*tert*-Butylpyridine, Ru(CO)(*t*-Bu_2OH-TPP)(*t*-Bupy). The reaction time was 26 h. Activity I alumina was used for the chromatography. Impurities were eluted with C_2HCl_3, and the product was eluted with 1:1 C_2HCl_3–CH_2Cl_2. The product was eluted with 5:5:1 C_2HCl_3–CH_2Cl_2–THF: yield 48%; visible spectrum 421 (5.42), 538 (4.31), 574 (3.96); IR ν_{OH} 3750, ν_{CO} 1950 cm^{-1}; ^1H NMR 8.78 (s, pyrrole-H), 8.03, 7.82 (d, J = 1.9 Hz, *o*-H), 5.57 (s, *p*-OH), 1.64, 1.60 (s, *m*-*t*-Bu), 5.18 (d, *t*-Bupy β-H), 1.45 (d, *t*-Bupy α-H), 0.35 (s, *t*-Bu). Anal. Calcd for $C_{86}H_{105}N_5O_5$ Ru: C, 74.32; H, 7.62; N, 5.04. Found: C, 74.25; H, 7.52; N, 5.13.

Ruthenium Carbonyl Tetrakis(3,5-di-*tert*-butyl-4-methoxyphenyl)porphyrin 4-*tert*-Butylpyridine, Ru(CO)(*t*-Bu_2OMe-TPP)(*t*-Bupy). The reaction time was 26 h. Activity I alumina was used for the chromatography. Impurities were eluted with C_2HCl_3, and the product was eluted with 10:1 C_2HCl_3–THF: yield 70%; visible spectrum 418 (5.41), 536 (4.31), 574 (3.88); IR ν_{CO} 1890 cm^{-1}; ^1H NMR 8.75 (s, pyrrole-H), 8.14, 7.90 (d, J = 2.0 Hz, *o*-H), 3.95 (s, *p*-OMe), 1.63, 1.58 (s, *m*-*t*-Bu), 5.17 (d, *t*-Bupy β-H), 1.50 (d, *t*-Bupy α-H), 0.36 (s, *t*-Bupy *t*-Bu). Anal. Calcd for $C_{90}H_{113}N_5O_5Ru$: C, 74.76; H, 7.88; N, 4.84. Found: C, 74.63; H, 7.79; N, 4.88.

Indium Complexes. The indium complexes were prepared by the method reported for In(*p*-R-TPP)Cl[2,9] and chromatographed on activity III Baker 0537 alumina. After removal of the chromatographic solvent, the product was dissolved in 1,1,2,2-tetrachloroethane and boiled for 30 min to ensure conversion to the axial chloride form. The products were recrystallized from CH_2Cl_2/hexane. Chromatographic details and characterization data are given below.

Indium Tetrakis(3,5-dimethoxyphenyl)porphyrin Chloride, In(OMe_2-TPP)Cl. Impurities were eluted with C_2HCl_3, and the product was eluted with 2:1 C_2HCl_3–$CHCl_3$: yield 72%; visible spectrum 410 (sh, 4.71), 430 (5.82), 518 (sh, 3.53), 560 (4.41), 599 (3.76); ^1H NMR 9.20 (s, pyrrole H), 7.63, 7.27 (m, *o*-H), 6.94 (t, J = 2.3 Hz, *p*-H), 4.01, 3.95 (s, *m*-OMe). Anal. Calcd for $C_{52}H_{44}N_4O_8InCl$: C, 62.26; H. 4.42; N, 5.59; Cl, 3.58. Found: C, 62.26; H, 4.53; N, 5.54; Cl, 3.68.

Indium Tetrakis(3,4,5-trimethoxyphenyl)porphyrin Chloride, In(OMe_3-TPP)Cl. Impurities, followed by product, were eluted with $CHCl_3$: yield 77%; visible spectrum 412 (sh, 4.73), 433 (5.71), 523 (sh, 3.58), 562 (4.38), 602 (3.95); ^1H NMR 9.20 (s, pyrrole H), 7.67, 7.34 (d, J = 1.6 Hz, *o*-H), 4.02, 3.92 (s, *m*-OMe), 4.15 (s, *p*-OMe). Anal. Calcd for $C_{56}H_{52}N_4O_{12}InCl$: C, 59.88; H, 4.67; N, 4.99; Cl, 3.16. Found: C, 59.76; H, 4.73; N, 4.91; Cl, 3.41.

Titanyl Complexes. The titanyl complexes were prepared by the method reported for titanium octaethylporphyrin oxide,[10] purified by chromatography on alumina, and recrystallized from CH_2Cl_2/hexane. Chromatographic details and characterization data are given below.

Titanium Tetrakis(3,5-dimethoxyphenyl)porphyrin Oxide, TiO(OMe_2-TPP). Activity III alumina was used for chromatography. Impurities were eluted with benzene, and the product was eluted with 3:1 benzene–$CHCl_3$: yield 53%; visible spectrum 408 (sh, 4.73), 427 (5.70), 512 (sh, 3.50), 552 (4.44), 588 (3.39); IR ν_{TiO} 965 cm^{-1}; ^1H NMR 9.26 (s, pyrrole H), 7.72, 7.30 (m, *o*-H), 6.96 (t, J = 2.3 Hz, *p*-H), 4.02, 3.96 (s, *m*-OMe). Anal. Calcd for $C_{52}H_{44}N_4O_9Ti$: C, 68.12; H, 4.84; N, 6.11. Found: C, 68.01; H, 4.82; N, 6.07.

Titanium Tetrakis(3,4,5-trimethoxyphenyl)porphyrin Oxide, TiO(OMe_3-TPP). The crude product was chromatographed on activity IV alumina. Elution with benzene was continued until the purple free porphyrin band separated from the red titanyl complex band. The column was extruded, the red band physically separated, and the product extracted into $CHCl_3$: yield 38%; visible spectrum 410 (sh, 4.65), 430 (5.55), 515 (sh, 3.53), 553 (4.35), 593 (3.53); IR ν_{TiO} 970 cm^{-1}; ^1H NMR 9.25 (s, pyrrole H), 7.77, 7.37 (d, J = 1.6 Hz, *o*-H), 4.02, 3.93 (s, *m*-OMe), 4.16 (s, *p*-OMe). Anal. Calcd for $C_{56}H_{52}N_4O_{13}Ti$: C, 64.86; H, 5.06; N, 5.40. Found: C, 64.73; H, 5.15; N, 5.23.

Titanium Tetrakis(3,5-di-*tert*-butyl-4-hydroxyphenyl)porphyrin Oxide, TiO(*t*-Bu_2OH-TPP). Activity II alumina and benzene were used in the chromatography: yield 56%; visible spectrum 434 (5.63), 520 (sh, 3.63), 558 (4.35), 598 (4.08); IR ν_{OH} 3760, ν_{TiO} 970 cm^{-1}; ^1H NMR 9.30 (s, pyrrole H), 8.34, 7.96 (d, J = 1.9 Hz, *o*-H), 5.61 (s, *p*-OH), 1.70, 1.63 (s, *m*-*t*-Bu)., Anal. Calcd for $C_{76}H_{92}N_4O_5Ti$: C, 76.74; H, 7.80; N, 4.71. Found: C, 76.66; H, 7.91; N, 4.73.

Titanium Tetra(3,5-di-*tert*-butyl-4-methoxyphenyl)porphyrin Oxide, TiO(*t*-Bu_2OMe-TPP). Baker 0538 alumina, activity I, was used in the chromatography. Impurities including free porphyrin were eluted with benzene, and the complex was eluted with 1:1 benzene–$CHCl_3$: yield 60%; visible spectrum 407 (sh, 4.66), 430 (5.69), 519 (sh, 3.59), 556 (4.39), 595 (3.97); IR ν_{TiO} 950 cm^{-1}; ^1H NMR 9.30 (s, pyrrole H), 8.45, 8.05 (d, J = 2.0 Hz, *o*-H), 4.05 (s, *p*-OMe), 1.71, 1.63 (s, *m*-*t*-Bu). Anal. Calcd for $C_{80}H_{100}N_4O_5Ti$: C,77.14; H, 8.09; N, 4.50. Found: C, 76.91; H, 8.05; N, 4.44.

Gallium Complexes. Three complexes were prepared by the method reported for Ga(*p*-R-TPP)Cl.[3] Due to the insolubility of H_2(*t*-Bu_2OMe-TPP) in acetic acid, an alternate method was used to prepare Ga(*t*-Bu_2OMe-TPP)Cl as described below. The complexes were purified by chromatography on Baker 0537 alumina. The crude products were boiled in $C_2H_2Cl_4$ solution until the ^1H NMR spectrum showed a single pyrrole peak (1–3 h) and recrystallized from CH_2Cl_2/heptane. Chromatographic details and characterization data are given below.

Gallium Tetrakis(3,5-dimethoxyphenyl)porphyrin Chloride, Ga(OMe_2-TPP)Cl. Activity IV alumina was used for the chromatography. Impurities were eluted with C_2HCl_3, and the product was eluted with 4:1 C_2HCl_3–EtOH: yield 81%; visible spectrum 403 (sh, 4.62), 424 (5.83), 510 (sh, 3.80), 552 (4.40), 589 (3.40); ^1H NMR (0 °C, 3:1 $C_2H_2Cl_4$–C_2HCl_3) 9.24 (s, pyrrole H),

(7) Stoochnoff, B. A.; Benoiton, N. L. *Tetrahedron Lett.* **1973**, 21–4.
(8) Eaton, S. S.; Eaton, G. R. *Inorg. Chem.* **1977**, *16*, 72–5.
(9) Eaton, S. S.; Eaton, G. R. *J. Am. Chem. Soc.* **1975**, *97*, 3660–6.
(10) Fuhrhop, J.-H.; Kadish, K. M.; Davis, D. G. *J. Am. Chem. Soc.* **1973**, *95*, 5140–7.

Table I. Activation Energies for *t*-Bupy Exchange and Phenyl Ring Rotation[a]

porphyrin	E_a, kcal/mol	$\Delta G^{\ddagger}_{298}$, kcal/mol	$\Delta H^{\ddagger}$, kcal/mol	$\Delta S^{\ddagger}$, eu	log k_{343},[b] s^{-1}
		t-Bupy Exchange[c]			
Ru(CO)(OMe_2-TPP)(*t*-Bupy)	23.0 ± 1.4	19.4 ± 1.9	22.3 ± 1.4	9.6 ± 3.9	0.73
Ru(CO)(OMe_3-TPP)(*t*-Bupy)	21.4 ± 0.8	18.7 ± 0.8	20.7 ± 0.8	6.8 ± 2.1	1.14
Ru(CO)(*t*-Bu_2OH-TPP)(*t*-Bupy)	20.8 ± 1.4	18.1 ± 1.3	20.1 ± 1.1	6.7 ± 2.7	1.50
Ru(CO)(*t*-Bu_2OMe-TPP)(*t*-Bupy)	20.1 ± 0.8	18.0 ± 1.1	19.3 ± 0.8	4.6 ± 2.2	1.55
		Phenyl Ring Rotation[d]			
Ru(CO)(OMe_2-TPP)(*t*-Bupy)	18.2 ± 1.2	20.3 ± 1.6	17.5 ± 1.2	−7.4 ± 3.0	0.07
Ru(CO)(OMe_3-TPP)(*t*-Bupy)	20.5 ± 2.1	20.1 ± 2.7	19.7 ± 2.1	−1.4 ± 5.7	−0.01
Ru(CO)(*t*-Bu_2OH-TPP)(*t*-Bupy)	17.3 ± 1.6	19.3 ± 2.0	16.6 ± 1.6	−9.3 ± 3.2	0.23
Ru(CO)(*t*-Bu_2OMe-TPP)(*t*-Bupy)	17.9 ± 1.3	19.4 ± 1.3	17.1 ± 1.3	−7.7 ± 2.9	0.26
In(OMe_2-TPP)Cl	16.2 ± 0.7	18.0 ± 0.8	15.4 ± 0.7	−8.7 ± 2.0	1.13
In(OMe_3-TPP)Cl	17.3 ± 0.8	18.2 ± 0.8	16.6 ± 0.8	−5.4 ± 2.1	1.09
TiO(OMe_2-TPP)	15.0 ± 0.6	17.4 ± 0.8	14.3 ± 0.6	−10.3 ± 1.8	1.48
TiO(OMe_3-TPP)	15.4 ± 0.2	17.4 ± 0.8	14.7 ± 0.6	−9.3 ± 1.8	1.44
TiO(*t*-Bu_2OH-TPP)	13.9 ± 0.7	16.6 ± 0.7	13.2 ± 0.7	−11.5 ± 2.2	1.92
TiO(*t*-Bu_2OMe-TPP)	14.2 ± 0.6	16.8 ± 0.8	13.5 ± 0.6	−11.2 ± 1.7	1.79
Ga(OMe_2-TPP)Cl[e]	14.1 ± 0.6	16.0 ± 0.8	13.5 ± 0.6	−8.5 ± 1.9	2.38
Ga(OMe_3-TPP)Cl[e]	12.8 ± 0.7	15.9 ± 0.8	12.2 ± 0.7	−12.3 ± 1.9	2.38
Ga(*t*-Bu_2OH-TPP)Cl[e]	12.3 ± 0.6	15.1 ± 0.8	11.7 ± 0.6	−11.4 ± 1.9	2.90
Ga(*t*-Bu_2OMe-TPP)Cl[e]	12.6 ± 0.5	15.4 ± 0.8	12.0 ± 0.5	−11.4 ± 1.9	2.71

[a] In 1,1,2,2-tetrachloroethane solution unless otherwise noted. Uncertainties are given as ±3 standard deviations from the least-squares line. [b] Rates for phenyl ring rotation in the ruthenium complexes were obtained by extrapolation, giving uncertainties of about 20%. Uncertainties in rates for other processes are about 5–10%. [c] Rates obtained in the presence of 1.0–1.5 equiv of *t*-Bupy. [d] Based on combined data from ortho protons and meta substituents. [e] In 3:1 1,1,2,2-tetrachloroethane–1,1,2-trichloroethylene solution.

7.30, 7.54 (m, *o*-H), 6.92 (t, J = 2.3 Hz, *p*-H), 3.95, 3.98 (s, *m*-OMe). Anal. Calcd for $C_{52}H_{44}N_4O_8GaCl$: C, 65.19; H, 4.63; N, 5.85; Cl, 3.70. Found: C, 64.93; H, 4.61; N, 5.84; Cl, 3.79.

Gallium Tetrakis(3,4,5-trimethoxyphenyl)porphyrin Chloride, Ga(OMe_3-TPP)Cl. Activity IV alumina was used for the chromatography. Impurities were eluted with CH_2Cl_2, and the product was eluted with 3:1 CH_2Cl_2–hexane: yield 82%; visible spectrum 407 (sh, 4.68), 427 (5.71), 515 (sh, 3.54), 553 (4.38), 592 (3.61); ^{1}H NMR (15 °C, 3:1 $C_2H_2Cl_4$–C_2HCl_3) 9.23 (s, pyrrole H), 7.62, 7.35 (d, J = 1.6 Hz, *o*-H), 4.00, 3.93 (s, *m*-OMe), 4.15 (s, *p*-OMe). Anal. Calcd for $C_{56}H_{52}N_4O_{12}GaCl$: C, 62.38; H, 4.86; N, 5.20; Cl, 3.29. Found: C, 62.09; H, 4.80; N, 5.09; Cl, 3.57.

Gallium Tetrakis(3,5-di-*tert*-butyl-4-hydroxyphenyl)porphyrin Chloride, Ga(*t*-Bu_2OH-TPP)Cl. Activity III alumina was used for the chromatography. Impurities were eluted with C_2HCl_3, and the product was eluted with 2:1 C_2HCl_3–CH_2Cl_2: yield 80%; visible spectrum 410 (sh, 4.55), 430 (5.66), 521 (sh, 3.55), 556 (4.26), 598 (4.02); IR ν_{OH} 3780 cm^{-1}; ^{1}H NMR (−14 °C, 3:1 $C_2H_2Cl_4$–C_2HCl_3) 9.20 (s, pyrrole H), 8.19, 7.92 (d, J = 1.9 Hz, *o*-H), 5.58 (s, *p*-OH), 1.66, 1.61 (s, *m*-*t*-Bu). Anal. Calcd for $C_{76}H_{92}N_4O_4GaCl$: C, 74.17; H, 7.54; N, 4.55; Cl, 2.88. Found: C, 74.14; H, 7.33; N, 4.62; Cl, 3.23.

Gallium Tetrakis(3,5-di-*tert*-butyl-4-methoxyphenyl)porphyrin Chloride, Ga(*t*-Bu_2OMe-TPP)Cl. The complex was prepared by refluxing 0.32 g of H_2(*t*-Bu_2OMe-TPP) and 0.17 g of $GaCl_3$ in 150 mL of 1:1 toluene–pyridine for 48 h. The crude product was chromatographed on activity III alumina. Unreacted porphyrin was eluted with benzene, and the product was eluted with $CHCl_3$. The product was treated with $C_2H_2Cl_4$ to effect conversion to the axial chloride and recrystallized from CH_2Cl_2/heptane: yield 49%; visible spectrum 427 (5.69), 516 (sh, 3.44), 555 (4.24), 595 (3.86); ^{1}H NMR (−16 °C, 3:1 $C_2H_2Cl_4$–C_2HCl_3) 9.23 (s, pyrrole H), 8.29, 8.00 (d, J = 2.0 Hz, *o*-H), 4.03 (s, *p*-OMe), 1.65, 1.59 (s, *m*-*t*-Bu). Anal. Calcd for $C_{80}H_{100}N_4O_4GaCl$: C, 74.69; H, 7.83; N, 5.35. Found: C, 74.76; H, 7.74; N, 4.46.

NMR Spectra. ^{1}H NMR spectra were run on samples that had been freshly prepared in a nitrogen atmosphere with concentrations of ca. (2–3) × 10^{-2} M. Our previous studies showed that rates of phenyl ring rotation and rates of *t*-Bupy exchange are independent of concentration.[2,8] Temperatures were calibrated after obtaining each set of data with methanol and ethylene glycol standards and the temperature-dependent chemical shifts of Van Geet.[11] Temperature calibrations were reproducible to ±0.5 °C. Temperatures are considered accurate to ±1.0 °C.

Slow- and fast-exchange data were analyzed to determine the temperature dependence of chemical shifts and line widths.[2] Computer simulated spectra were obtained by using DNMR3A[12] for the spin-coupled ortho protons on the phenyl rings and EXCNMR[13] for the two-site exchange of the meta substituents (methoxy or *tert*-butyl groups) and for the two-site exchange of the *tert*-butyl groups on free and coordinated *t*-Bupy.

Rate constants were obtained by visual comparison of calculated and observed spectra and are accurate within 5–10% except near the slow- and fast-exchange limits where uncertainties are about 20%. In all cases the rates obtained from the spectra of the ortho protons and of the meta substituents agreed within experimental uncertainty. Activation parameters were determined from weighted (according to uncertainty) least-squares fits to the Arrhenius (ln k_r vs. $1/T$) and the Eyring [ln (hk_r/kT) vs. $1/T$] equations. The number of data points and the size of the temperature range over which data were taken for the various classes of compounds are as follows: ruthenium complexes, for ortho protons, 9–12 points, 50–60 °C range, for meta groups, 6–8 points, 35–40 °C range, for *t*-Bupy exchange, 10–15 points, 60–85 °C range; indium complexes, for ortho protons, 14–15 points, 80–90 °C range, for meta groups, 9 points, 50–55 °C range; titanyl complexes, for ortho protons, 14–17 points, 85–100 °C range, for meta groups, 7–10 points, 35–55 °C range; gallium complexes, for ortho protons, 13–15 points, 85–90 °C range, for meta groups, 8–9 points, 40–55 °C range. The slow rate of ring rotation, the small chemical shift difference for the meta substituents, and the boiling point of $C_2H_2Cl_4$ limited the data which could be obtained for Ru(CO)(OMe_2-TPP)(*t*-Bupy) and Ru(CO)(OMe_3-TPP)(*t*-Bupy). The activation parameters for these two complexes are more uncertain than those for the other cases examined. Data for the ortho protons and meta substituents were combined to obtain the activation parameters which are reported in Table I. Uncertainties are given as ±3 standard deviations. However, we have previously shown that the reproducibility of activation parameters obtained on similar systems is considerably better than that indicated by our stated uncertainties of ±3 standard deviations.[2,8]

(11) Van Geet, A. L. *Anal. Chem.* **1968**, *40*, 2227–9.

(12) Bushweller, C. H.; Bhat, G.; Letendre, L. J.; Brunelle, J. A.; Bilofsky, H. S.; Ruben, H.; Templeton, D. H.; Zalkin, A. *J. Am. Chem. Soc.* **1975**, *97*, 65–73.

(13) Kreiger, J., Ph.D. Thesis, Massachusetts Institute of Technology, 1971. Lisle, J. S., S.B. Thesis, Massachusetts Institute of Technology, 1968. Whitesides, G. M.; Fleming, J. S. *J. Am. Chem. Soc.* **1967**, *89*, 2855–9.

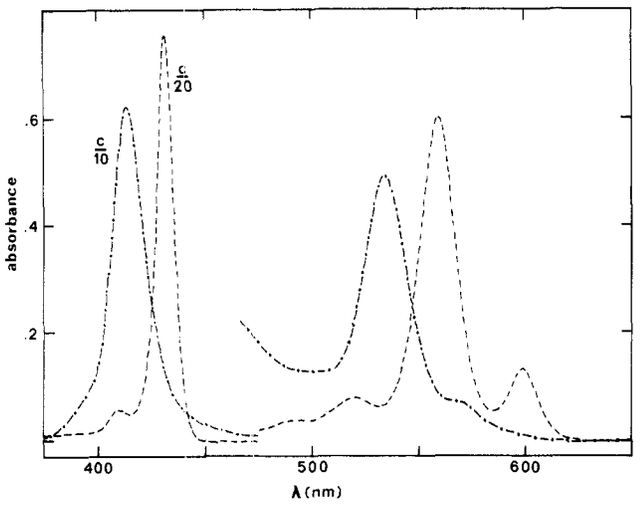

Figure 1. Visible spectra of 2.36×10^{-5} M In(OMe_2-TPP)Cl (---) and 2.26×10^{-5}M Ru(CO)(OMe_2-TPP)(*t*-Bupy) (-·-) in $CHCl_3$ solution at room temperature. Spectra from 375 to 475 nm were obtained with the solutions diluted by the factors noted beside the traces.

In the following discussion, rates at 70 °C are used for comparison of the complexes. This temperature was chosen because it falls within, or close to, the intermediate exchange region for most of the complexes. However, similar trends were also observed at 20 and 50 °C.

Results and Discussion

Electronic Spectra. The electronic spectra of the "normal" metalloporphyrins consist of an intense band near 420 nm (Soret band) and two bands between 500 and 600 nm (α and β bands).[14] The spectra reported in the Experimental Section all fit this general pattern. However, the transition energies and relative intensities of the α and β bands vary considerably as a function of metal ion and phenyl ring substituent (cf. Figure 1). Gouterman et al. have shown that shifts in the transition energies and relative intensities of the α and β bands in tin octaethylporphyrin dihalides (halide = F, Cl, Br, and I) correlate with changes in the electron density in the porphyrin ring obtained from extended Hückel calculations.[15] Similarly, the visible spectra of a series of Zn(TPP)L and $Zn(TPP)X^-$ complexes exhibit changes in transition energies and relative band intensities which depend on the charge and polarizability of the axial ligand.[16] Analogous changes in the visible spectra of free porphyrins as a function of phenyl ring substituent have also been observed.[17] In each of these cases a correlation between the ratio $\epsilon_\alpha/\epsilon_\beta$ and the energy of the α band (ν_α) was observed. In Figure 2 the values of $\epsilon_\alpha/\epsilon_\beta$ are plotted against ν_α for the meta- and para-substituted ruthenium, indium, titanyl and gallium complexes which are reported in this paper and in ref 2, 3, and 8. The points for the ruthenium complexes fall on a different line than the points for the other metal ions. If the indium complexes are considered separately, a slightly different line is obtained. However, the difference between indium and gallium or titanyl is small for the purposes of this paper. The line obtained for the zinc complexes in ref 16 falls to the left of the lines in Figure 2 and is less steeply sloped. Although the metal

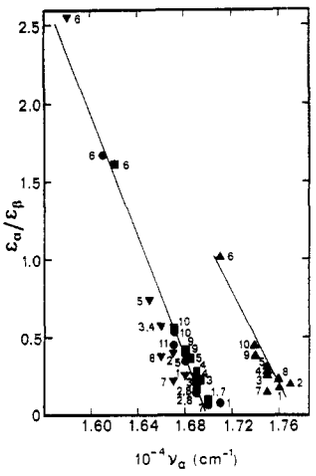

Figure 2. Plot of the ratio of the intensities of the α and β transitions ($\epsilon_\alpha/\epsilon_\beta$) vs. the energy of the α transition in the visible spectra of the metalloporphyrins in chloroform solution at room temperature. Metal ions are denoted as follows: ▲, MXY = Ru(CO)(*t*-Bupy); ●, MXY = TiO; inverted triangle, MXY = InCl; ■, MXY = GaCl. Ring substituents are labeled as follows: 1, 4-CF_3; 2, 4-Cl; 3, 4-Me; 4, 4-*i*-Pr; 5, 4-OMe; 6, 4-Et_2N; 7, 3,5-$(OMe)_2$; 8, 3,4,5-$(OMe)_3$; 9, 3,5-*t*-Bu_2-4-(OMe); 10, 3,5-*t*-Bu_2-4-OH; 11, 4-OH.

ion influences the correlation, similar correlations are evident for the effects of the axial ligand and the phenyl ring sustituent on the electronic spectra. Bulky ortho substituents have also been found to have a steric effect on ν_α and $\epsilon_\alpha/\epsilon_\beta$ in free porphyrins.[17] The bulky ortho substituents result in points which are substantially to the left of the line obtained for the para-substituted porphyrins.[17] The points for the meta-substituted metalloporphyrins in Figure 2 fall close to the lines obtained for the para-substituted metalloporphyrins. Thus the steric effects of the meta substituents on the electronic spectra appear to be small, and it seems reasonable to use the electronic spectra of the metalloporphyrins to monitor the electronic effects of the meta substituents.

^{1}H NMR Spectra. Crystallographic results have shown that in metal complexes of tetraphenylporphyrins the dihedral angle between the plane of the porphyrin ring and the plane of the phenyl ring is typically between 60 and 90°.[18] When the ligands (X, Y) on the two sides of the metalloporphyrin plane are different, the groups in the ortho and meta positions of the phenyl ring (cf. 1) are pairwise nonequivalent provided that exchange of ligands X and Y is slow on the NMR time scale. The slow-exchange ^{1}H NMR spectra of these symmetrically substituted porphyrins gave AB patterns for the ortho protons with J = 1.6–2.0 Hz except for MXY(OMe_2-TPP) where coupling to the para proton gave an ABC pattern. Two singlets were observed for the nonequivalent *m*-methoxy or *m*-*tert*-butyl groups. There is no resolved coupling between the ortho protons and the methoxy or *tert*-butyl protons. The chemical shift differences between nonequivalent ortho protons ranged from a low of 20 Hz in Ru(CO)(OMe_3-TPP)(*t*-Bupy) to a high of 42 Hz in TiO-(OMe_2-TPP). Chemical shift differences between nonequivalent meta substituents ranged from a low of 2 Hz in Ru(CO)(OMe_2-TPP)(*t*-Bupy) to a high of 10 Hz in In-(OMe_3-TPP)Cl. Variable-temperature spectra were obtained in 1,1,2,2-tetrachloroethane ($C_2H_2Cl_4$) solution for MXY = TiO, InCl, and Ru(CO)(*t*-Bupy) and in 3:1 $C_2H_2Cl_4$–C_2HCl_3 solution for MXY = GaCl. As the temperature was raised the signals for the nonequivalent ortho protons broadened and averaged to a single line [a doublet

(14) Gouterman, M. In "The Porphyrins"; D. Dolphin, Ed.; Academic Press: New York, Vol. III, pp 1–165, 1978.
(15) Gouterman, M.; Schwarz, F. P.; Smith, P. D.; Dolphin, D. *J. Chem. Phys.* **1973**, *59*, 676–90.
(16) Nappa, M.; Valentine, J. S. *J. Am. Chem. Soc.* **1978**, *100*, 5075–80.
(17) Moet-Ner, M.; Adler, A. D. *J. Am. Chem. Soc.* **1975**, *97*, 5107–11.
(18) Hoard, J. L. *Ann. N.Y. Acad. Sci.* **1973**, *206*, 18–31.

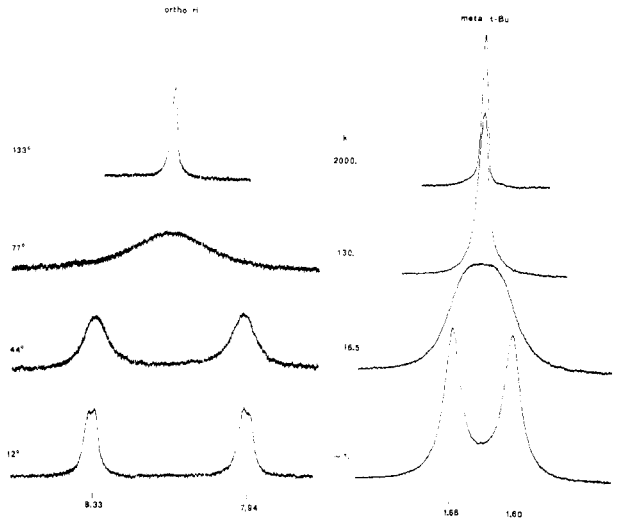

Figure 3. Variable-temperature ^1H NMR spectra of the ortho protons and meta *tert*-butyl groups of TiO(*t*-Bu_2OH-TPP) in 1,1,2,2-tetrachloroethane solution. Chemical shifts are in parts per million from Me_4Si. Rate constants for phenyl ring rotation (k, s^{-1}) were obtained by computer simulation as described in the text. Simulated spectra are superimposable on the experimental spectra.

for MXY(OMe$_2$-TPP)] while the signals for the meta substituents also coalesced to a singlet. The variable-temperature NMR spectra of TiO(*t*-Bu_2OH-TPP) (Figure 3) are typical spectra. All line-shape changes were reversible with temperature. We have previously shown that for substituted tetraphenylporphyrin complexes with MXY = Ru(CO)(*t*-Bupy), InCl, TiO, and GaCl, in the absence of excess axial ligand, the averaging of resonances for nonequivalent phenyl protons is due to phenyl ring rotation and not due to interchange of the axial ligands (X, Y) bound to the metal ion.[3,9] For the ruthenium carbonyl porphyrins, coordinated *t*-Bupy exchanges with *t*-Bupy free in solution but does not replace the carbonyl ligand. The *t*-Bupy exchange does not average the nonequivalent ortho or meta signals and may be examined as an independent process by monitoring the 4-*tert*-butyl signals, although it occurs at about the same rate as phenyl ring rotation. Thus the kinetic data obtained by computer simulation of the variable-temperature NMR spectra can be used to determine the activation parameters for both phenyl ring rotation and *t*-Bupy exchange.

Activation Parameters. Rates of phenyl ring rotation were obtained by computer simulation of the spectra for the ortho protons and meta substituents. Since the chemical shift differences between the resonances for the methoxy substituents were substantially smaller than those for the ortho protons, useful kinetic data were obtained over a smaller temperature range than that for the ortho protons (see Experimental Section and Figure 3). In all cases the rates of phenyl ring rotation obtained from the ortho and meta resonances at the same temperature agreed within experimental error. Rates of exchange between free and coordinated *t*-Bupy were obtained by computer simulation of the signals for the 4-*tert*-butyl groups. Activation parameters for phenyl ring rotation were obtained from the combined data for the ortho protons and meta substituents. The values of the activation parameters are in Table I with uncertainties given as ±3 standard deviations. In all cases, correlation coefficients of 0.995 or better were obtained, and there was no evidence of deviation from linearity.

Relative Effect of Various Substituents. The experimental results discussed above clearly establish that

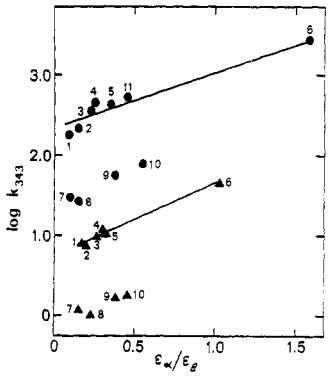

Figure 4. Plot of the rate of phenyl ring rotation at 343 K vs. the ratio of the intensities of the α and β transitions observed in the visible spectra: ▲, MXY = Ru(CO)(*t*-Bupy); ●, MXY = TiO. Lines are least-squares fits to the data for the para-substituted porphyrins. Ring substituents are labeled as in Figure 2.

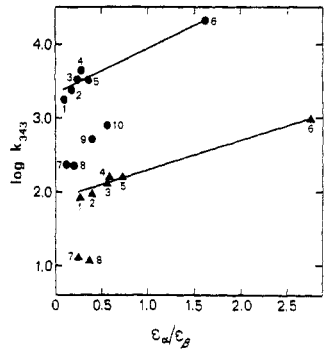

Figure 5. Plot of the rate of phenyl ring rotation at 343 K vs. the ratio of the intensities of the α and β transitions observed in the visible spectra: ▲, MXY = InCl; ●, MXY = GaCl. Lines are least-squares fits to the data for the para-substituted porphyrins. Ring substituents are labeled as in Figure 2.

the rate of ring rotation in metallotetraphenylporphyrins depends upon the phenyl ring substituent and on the metal. We seek an explanation of the observed dependence in terms of the bonding interactions (electronic effects) and nonbonded interactions (steric effects) within the molecule. That these are not fully separable concepts is well illustrated by the effect of the metal, as discussed previously.[2,3,9] Since the reactions were studied in solution, the effect of solvent could also be important. Our discussion of each factor individually should not be construed as a failure to recognize the intimate interconnection between electronic effects, steric effects, and solvation effects.

As discussed above, comparison of the electronic spectra of the porphyrin complexes provides a useful monitor of the electronic effects of both the meta and para substituents on the phenyl rings. In Figures 4 and 5 the rates of phenyl ring rotation for the ruthenium, titanyl, indium, and gallium complexes reported here and in ref 2, 3, and 9 are plotted vs. $\epsilon_\alpha/\epsilon_\beta$, the ratio of the extinction coefficients for two of the electronic transitions. The rates for the para-substituted complexes yield a reasonably good linear correlation with the electronic effect of the substituent as monitored by $\epsilon_\alpha/\epsilon_\beta$. However, in each case the rates for the meta-substituted complex are slower than would be expected if the rates were dictated by the electronic effects operative in the para-substituted complexes. Thus it is evident that other factors, such as steric effects on the transition state, which are not monitored by the $\epsilon_\alpha/\epsilon_\beta$ ratio are more important for the meta-substituted complexes than for the para-substituted complexes.

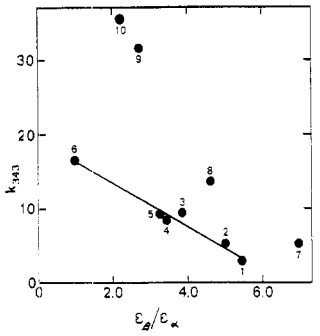

Figure 6. Plot of the rate of exchange between free and coordinated *t*-Bupy at 343 K vs. the ratio of the intensities of the β and α transitions observed in the visible spectra for MXY = Ru(CO)(*t*-Bupy). The line is the least-squares fit to the data for the para-substituted porphyrins. Ring substituents are labeled as in Figure 2.

In Figure 6 the rate of *t*-Bupy exchange in the ruthenium complexes is plotted vs. $\epsilon_\beta/\epsilon_\alpha$ for the complexes reported here and in ref 8. The rates for the meta-substituted complexes are much faster than would be expected on the basis of the electronic effects as monitored by the linear correlation of rate with the electronic effects of the para substituents. This observation is consistent with a steric contribution of the meta substituent to the lability of the axial ligand.

Both the decreased rate of ring rotation and the increased rate of axial ligand exchange are in the direction which could also be consistent with a specific solvation model. In the range of solvents in which adequate NMR spectra were obtainable, no more than about a factor of 2 variation in these rates was found for various solvents.[2] It seems implausible that the variety of solvents used would have such similar effects if specific solvation were the dominant factor in these experiments. However, in solution studies the concept of steric effects on dynamic processes is not separable from the concept of solvent effects. Lacking a testable hypothesis here, we include within the concept of steric effects any changes in solvation due to different sizes of the substituents.

Comparison with Prior Studies of Steric Effects of Meta Substituents. The calculations of Wolberg indicated that restricted rotation of the phenyl rings in metallotetraphenylporphyrins was due predominately to nonbonded interaction between the ortho hydrogen on the phenyl ring and the pyrrole hydrogen.[19] The calculations were done by assuming a hydrogen in the meta position, but inspection of molecular models indicates that the conclusion remains valid even with larger meta substituents. Consequently, the steric effect of the meta sustituent appears to be indirect, via its effect on the ortho hydrogen. Such effects have been called "buttressing" effects. Of particular note is our observation that *m*-methoxy and *m*-*tert*-butyl groups have similar impacts on ring rotation rates despite the fact that the *tert*-butyl group is by most criteria more sterically demanding than the methoxy group. In contrast, the *m*-*tert*-butyl group accelerates axial ligand exchange more than does the methoxy group.

Gust observed a buttressing effect of the substituent X on the rate of phenyl ring rotation in pentaarylbenzenes **2**.[20] The barrier to rotation of the tolyl groups increased as the size of X increased.[20] Charton's regression analysis of the buttressing effect on racemization of substituted biphenyls **3** indicated that the buttressing effect of the

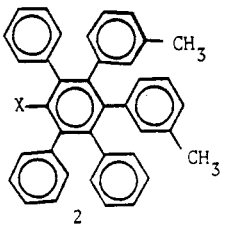

2

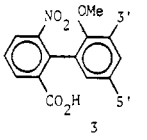

3

3′-substituent depended on its size.[21] In both of these studies the ortho substituent was a bulky group (phenyl or methoxy). However, in the metallotetraphenylporphyrins used in the present study the ortho substituent was hydrogen. The ortho hydrogen senses the dimension of the meta substituent close to the phenyl ring, not the overall size of the group. Thus it is necessary to examine in detail the conformations of the meta substituents.

Experimental and calculational studies have indicated that in the absence of steric or electronic constraints due to other substituents, a methoxy substituent on an aromatic ring prefers the conformation in which the O and C of the methoxy lie in the plane of the aromatic ring.[22,23] Rotation about the ring–oxygen bond is facile when the substituents ortho to the methoxy group are both hydrogens. Thus in MXY(OMe_2-TPP) the ortho hydrogens sense either the CH_3 or the lone pairs of the in-plane methoxy group. In 3,4,5-trimethoxy-substituted benzene rings the 4-methoxy group is forced to a perpendicular orientation, and the 3,5-methoxy groups have the CH_3 groups oriented toward the 2,6-hydrogens.[22,24] Thus in MXY(OMe_3-TPP) both ortho hydrogens interact with the CH_3 group of the *m*-methoxy substituents.

In the 2,6-di-*tert*-butylphenol the hydroxy group is coplanar with the benzene ring, but in 2,6-di-*tert*-butylanisole the methoxy group is forced to adopt a perpendicular conformation.[25] The finding that the hydroxy group can retain a planar conformation with the hydrogen directed toward an adjacent *tert*-butyl group is a striking example of the specificity of steric effects. The steric effect of a particular substituent can be sensed quite differently by two different substituents.

In view of these conformations, the relative sizes of the methoxy and *tert*-butyl groups may not be very different when sensed by the ortho hydrogen. Consequently, the buttressing effect of the methoxy and *tert*-butyl groups on ring rotation could be similar. In contrast, the steric effect on axial ligand exchange would likely be more nearly proportional to the total volume of the substituent, which is consistent with our results.

Charton did not find a dependence of the rate of racemization of biphenyls **3** on the size of the 5′-substituent (size was estimated from van der Walls radii) and concluded that the 5′-substituent did not have a buttressing effect.[21] However, since the 6′-substituent was hydrogen, the usual measures of steric size may not be relevant for the interaction of the 5′- and 6′-substituents.

(19) Wolberg, A., *J. Mol. Struct.* **1974**, *21*, 61–6.
(20) Patton, A.; Dirks, J. A.; Gust, D. *J. Org. Chem.* **1979**, *44*, 4749–52.
(21) Charton, M. *J. Org. Chem.* **1977**, *42*, 2528–9.
(22) Anderson, G. M., III; Kollman, P. A.; Domelsmith, L. N.; Houk, K. N. *J. Am. Chem. Soc.* **1979**, *101*, 2344–52 and references therein.
(23) Hofer, O. *Monatsh. Chem.* **1978**, *109*, 405–19.
(24) Koetzle, T. F.; Williams, G. J. B. *J. Am. Chem. Soc.* **1976**, *98*, 2074–8.
(25) Allinger, N. L; Maul, J. J.; Kickey, M. J. *J. Org. Chem.* **1971**, *36*, 2747–52.

Effect of Metal. The metal can also influence the rate of ring rotation by both electronic and steric interactions. That there are electronic effects due to interaction of the metal orbitals with porphyrin orbitals is obvious but is difficult to quantitate. Apparently of more importance in the series of compounds studied here is the indirect steric effect that results from porphyrin ring distortion to satisfy the preferred metal–nitrogen bond length.[2,3] The steric effects of the meta substituents on phenyl ring rotation are of comparable magnitude for the four metal ions examined.

Acknowledgment is made to the donors of the Petroleum Research Fund, administered by the American Chemical Society, for partial support of this work. Elemental analyses were performed by Spang Microanalytical Laboratory.

Registry No. $H_2(OMe_2$-TPP), 74684-34-7; $H_2(OMe_3$-TPP), 74684-35-8; $H_2(t$-Bu_2OH-TPP), 74684-36-9; $H_2(t$-Bu_2OMe-TPP), 74684-37-0; Ru(CO)(OMe_2-TPP)(*t*-Bupy), 74684-73-4; Ru(CO)(OMe_3-TPP)(*t*-Bupy), 74684-74-5; Ru(CO)(*t*-Bu_2OH-TPP)(*t*-Bupy), 74684-75-6; Ru(CO)(*t*-Bu_2OMe-TPP)(*t*-Bupy), 74684-76-7; In(OMe_2-TPP)Cl, 74684-77-8; In(OMe_3-TPP)Cl, 74684-78-9; TiO(OMe_2-TPP), 74684-79-0; TiO(OMe_3-TPP), 74709-67-4; TiO(*t*-Bu_2OH-TPP), 74709-68-5; TiO(*t*-Bu_2OMe-TPP), 74709-69-6; Ga(OMe_2-TPP)Cl, 74684-80-3; Ga(OMe_3-TPP)Cl, 74684-81-4; Ga(*t*-Bu_2OH)-TPP)Cl, 74684-82-5; Ga(*t*-Bu_2OMe-TPP)Cl, 74709-70-9; pyrrole, 109-97-7; 3,5-dimethoxybenzaldehyde, 7311-34-4; 3,4,5-trimethoxybenzaldehyde, 86-81-7; 3,5-*tert*-butyl-4-hydroxybenzaldehyde, 1620-98-0; 3,5-di-*tert*-butyl-4-methoxybenzaldehyde, 74684-38-1.

Mechanism of Cyclization of 2-Azido-3-benzoyl Enamines to 5-Phenacyltetrazoles: Rate-Limiting Proton Transfer and Iminium Ion Isomerization

Edward P. Ahern, Kieran J. Dignam, and A. F. Hegarty*[1]

Chemistry Department, University College, Cork, Ireland

Received February 5, 1980

The unusual stability of the azides **5** has been investigated; these are shown to exist as the enamine tautomer **5b**. The rates of cyclization of the azides **5b** and **14** to the corresponding tetrazoles **4b** and **4c** (in water at 25 °C) vary in a complex way with pH, displaying both acid catalysis and inhibition at pH <6 and base catalysis at pH >9. A "bell-shaped" dependency of k_{obsd} on pH is observed with a maximum at pH 2.1. These results are interpreted as follows: at moderate acidities ($2 < pH < 6$) proton transfer to **5b** is the slow step, subsequent isomerization of the protonated species **7Z** and cyclization (**9E** → **4b**) being rapid. General-acid catalysis (Brønsted $\alpha = 0.57$, $k_{HOAc}/k_{DOAc} = 6.9$) is observed, but the rate-determining step can be changed at high buffer concentration (as shown by nonlinear k_{obsd} vs. [buffer] plots) or at low pH to a *Z*/*E* isomerization about the >C=$^+$N< bond of the protonated enamine (to give **7E**). Deprotonation of the latter gives (*E*)-imidoyl azide **9E** which rapidly cyclizes. The azide group therefore acts as an efficient internal trap for the imine group; only the isomer in which the lone pair on nitrogen is cis to the azide cyclizes to the tetrazole.

The existence of a tautomeric equilibrium between azidoazomethine derivatives and their corresponding tetrazoles has been established for some time.[2] In most cases the tetrazole form (**2**) is the more stable although a number of heterocyclic and acyclic azides, **1**, are known which are stable at room temperature.

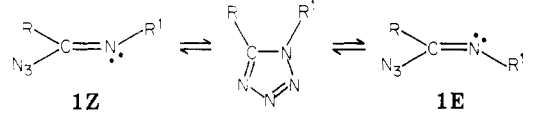

1Z ⇌ **2** ⇌ **1E**

The mechanism of isomerization of **1** → **2** has been investigated by a number of authors.[3] The most recent report by Leroy et al.[4] is based on a theoretical study of the energy factors involved in the cyclization. Of particular interest is the small energy of activation for the reaction and the far higher stability predicted for the tetrazole isomer. It is suggested that the driving force for cyclization is provided by the movement of the lone pair of electrons on the imidoyl nitrogen toward the terminal nitrogen of the azide group. A subsequent study of the vinyl azide–υ-triazole isomerization[5] shows that a π system can also participate directly in the formation of the σ bond between carbon and the terminal azido nitrogen. However, a much higher activation energy (42.9 kcal/mol as against 12.6 kcal/mol) was calculated for the neutral substrate relative to the vinyl azide anion.

Several factors govern both the rate of isomerization of azide → tetrazole[6] and the equilibrium position. Electron-withdrawing substituents, higher temperatures, and an acidic medium tend to favor the azide form. Moreover, it has recently been shown,[7] in line with the theoretical finding of Leroy, that only one of the possible imidoyl azide isomers, i.e., that in which the lone pair and the azide group are cis (**1Z**), will cyclize. This isomerization step (**1E** → **1Z**) may then be rate determining for the conversion of the azide to the tetrazole.

(1) To whom correspondence should be addressed at the Chemistry Department, University College, Belfield, Dublin 4, Ireland.

(2) Lwowski, W. "The Chemistry of the Azido Group"; Patai, S., Ed., Interscience: New York, 1973; p 503.

(3) Reimlinger, H. *Chem. Ber.* **1970**, *103*, 1900. Elguero, J. *Bull. Soc. Chim. Fr.* **1971**, 1925. Reynolds, G. A.; Van Allan, J. A.; Tinker, J. F. *J. Org. Chem.* **1959**, *24*, 1205.

(4) Burke, L. A.; Elguero, J.; Leroy, G.; Sana, M. *J. Am. Chem. Soc.* **1976**, *98*, 1685.

(5) Burke, L. A.; Leroy, G.; Nguyen, M. T.; Sana, M. *J. Am. Chem. Soc.* **1978**, *100*, 3668.

(6) Butler, R. N. *Adv. Heterocycl. Chem.* **1977**, *21*, 402.

(7) Hegarty, A. F.; Brady, K.; Mullane, M. *J. Chem. Soc., Chem. Commun.* **1978**, 871.

0022-3263/80/1945-4302$01.00/0